

# Optical Lithographic Performance and Resolution Using Strong Dark-Field Phase-Shifting of Discrete Patterns

John S. Petersen and David J. Gerold

Petersen Advanced Lithography, Inc. 8834 N. Capital of Texas Highway, Ste. 304, Austin, TX 78759  
Email: [jpetersen@advlitho.com](mailto:jpetersen@advlitho.com) Phone: (512)241-1100 Web: <http://advlitho.com>

## Abstract

Today, non-optical lithographic techniques are used to image the smallest discrete gate patterns used to make advanced GaAs devices. These techniques are very powerful but have low throughput. With growing device demand, there is a need to make these small features with the more cost-effective optical lithography. This paper briefly discusses the physics of the imaging process for several optical imaging techniques that extend gate resolution and contrasts expected performance of the techniques.

The optical resolution limit of a discrete pattern is a function of the wavelength, the aberrations of the imaging system, the numerical aperture of the lens, the exposure source shape and size, and the type of mask and resists being used. Several optical techniques exist for making small images. The simplest technique uses two pairs of binary assist features and off-axis illumination to image positive-acting resists. This method can be a very powerful imaging technique, provided the exposure tool can use an off-axis source. Other techniques use phase-shifting of the diffraction pattern to build the aerial image. Dark-field weak phase-shifting techniques can be used with positive-acting photoresists, but the exposure-focus latitude is limited compared to the results of stronger phase-shifting techniques.

Phase-edge lithography exhibits the best imaging potential, with resolutions as small as one quarter of the ratio of the exposure wavelength and numerical aperture of the stepper, but requires a negative-tone or image reversal resist. Supply of these resists at I-line may be problematic and, because they use a thermally activated acid to drive a catalytic reaction, they may require extreme airborne base contamination control for peak performance. As an alternative, we propose using a dark-field strong phase-shifting technique that we call GaAsMask™.

This patent-pending method uses phase-shifted, sub-resolution assist features to shape the discrete feature's diffraction pattern, minimizing the electric field at zero spatial frequency and leaving two beams of light at the edge of the lens pupil plane to reconstruct the desired feature using two-beam interference. Two-beam interference improves depth of focus because as long as the beams maintain spatial

and temporal coherence the phase relationship required to reconstruct the image is maintained.

Figure 1 shows a diffraction pattern for a 240 nm isolated space for (A) a binary mask with no assists, (B) a strong phase shift mask, (C) a weak phase shift mask, and (D) a binary mask with assist features.

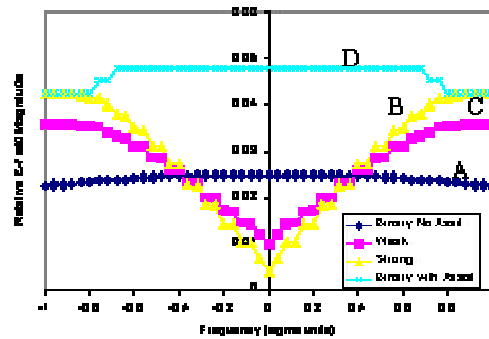


Figure 1: Diffraction Pattern

Figure 2 shows the aerial image for each of the diffraction patterns shown in Figure 1. In Figure 2 the binary assist is shown with both on-axis and off-axis quadrupole illumination. The difference in intensity between the binary and the phase-shift plates are due to the feature layout, which is described with the results.

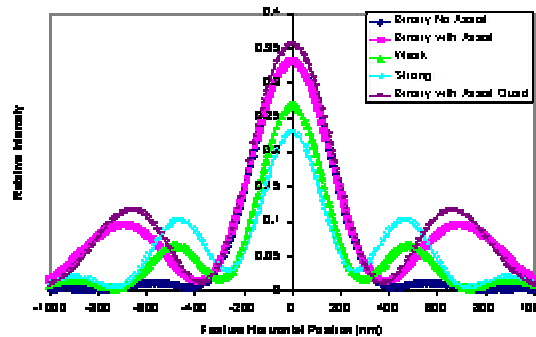


Figure 2: Inverse Fourier Transform, Squared is the Aerial Image.

The strong phase shift mask has the lowest intensity but the narrowest image width.

Projection lithography works in the Fraunhofer diffraction region. The diffraction pattern at this distance from the mask (object plane) can be described by the following Fourier transform. For a binary mask feature:

Equation 1<sup>[1]</sup>  

$$F\{m(x)\} = -T_P w_P \text{sinc}(\pi v w_P) + 2T_A w_A \cos(2\pi v \Delta x) \text{sinc}(\pi v w_A)$$

where:

T and W equal the complex transmittance and width of the primary feature, P, and assist feature, A,

v is spatial frequency,

$\Delta x$  is the distance from the center of the primary feature to the center of the assist feature, and

$\text{sinc}(x) = \sin(x)/x$ .

Phase-shifting can be examined simply by subtracting either the primary term, Equation 2, or the combined assist feature term, Equation 3.

Equation 2

$$F\{m(x)\} = T_P w_P \text{sinc}(\pi v w_P) + 2T_A w_A \cos(2\pi v \Delta x) \text{sinc}(\pi v w_A)$$

Equation 3

$$T_P w_P \text{sinc}(\pi v w_P) - 2T_A w_A \cos(2\pi v \Delta x) \text{sinc}(\pi v w_A)$$

Curve “D” in Figure 1 shows a graphical representation of the binary solution for equation 1. Curve “B” in figure 1 shows a phase-shift solution for Equation 3.

The frequency where the center of each node is located is driven by the distance  $\Delta x$ . The smaller this value, the greater the absolute frequency value. Figure 3 shows how the focus tolerance changes with nodal position in frequency space. In this figure, the vertical axis shows the percent exposure range about the dose to size a 130nm clear isolated feature with respect to frequency for varying amounts of defocus. Typically, for an exposure tool with 0.70 numerical aperture, 248nm exposure wavelength and partial coherence of 0.3, a process is said to be production worthy if the exposure latitude is greater than or equal to 5% and has a focus tolerance of more than 0.4 microns.

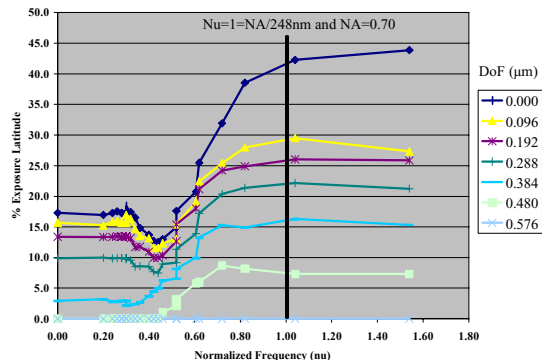


Figure 3: Exposure Latitude/ DoF for Different Depths of Focus

In Figure 3, this occurs when the normalized frequency is larger than 0.6, with optimum performance at frequencies between 0.8 and 1.2.

Below the frequency of 0.6, from 0 to 0.3 the performance is the same as an unmodified sinc function and the phase shifter provides no enhancement. Between frequencies of 0.3 and 0.6, the performance is worse than if no phase shifting was used. This degradation appears to be related to the introduction of 180-degree phase component of the node and the width of this phase region defined by the partial coherence of the imaging system. This phase component is not observed at frequencies greater than 0.92 for coherent light, but with partially coherent illumination it would be first introduced at frequency 0.92 minus 0.3, the coherence in this example. For a value of 0.62 the assist feature must be placed properly to remove any unwanted phase component.

To make a strong shifter, the sum of the complex transmittance and the width for the assist features is designed to cancel the electric field of the primary feature so that the resulting amplitude at zero frequency is zero. Equation 4 shows that for the simple case of one pair of assist features this occurs when:

Equation 4

$$T_P \cdot w_P = 2 \cdot T_A \cdot w_A$$

Further, the assist features are placed close enough to the primary feature to position the side-lobes of the Fourier transform at frequencies greater than 0.6 and less than or equal to a frequency defined in Equation 5:

Equation 5

$$v \leq \frac{(1 + \alpha \cdot \sigma) \cdot \Delta x \cdot NA}{\lambda}$$

where  $\sigma$  and NA equal, respectively, the partial coherence and numerical aperture of the exposure tool and  $\alpha$  is a factor bigger than one that takes into account the side-lobe's width as defined by the variables in Equations 2 and 3.

A strong phase-shifted type image forms by interfering the two lobes of the modified sinc function when they are brought back together at the image plane. Because the lobes are symmetric about the center of the optical axis the diffracted beams maintain a uniform interference relationship when equally aberrated, as in the case where the imaging material is moved in or out of the best image plane. This invariance in the interference relationship with focus gives rise to stability of the size and shape of the final resist image. In fact, with respect to spatial coherence, if the lobes were points with no radial distribution about their nodal centers, the depth of focus would be infinite. However, since the nodes are not points and energy distribution exists away

from the nodal center, the interference from these off center components reduces the focus tolerance to something less than infinite. However, focus tolerance is still significantly better than the depth of focus of a unmodified sinc function or of a modified function whose phase-shifted electric fields are not perfectly balanced. The nodal center frequency is also important. This is because using the numerical aperture of the lens as a low pass frequency filter reduces the degree of non-optimal interference that is associated with interfering beams that are not symmetric about the optical axis.

Figure 4 shows simulated exposure latitudes and depth-of-focus comparisons of a 240 nm isolated space imaged with and without 120nm assist features. Here,  $\Delta x$  is 300 nm and  $T_A$  is 1.0 for the strong shift, 0.5 for the weak shift, and 632 nm for the binary with assist features. The primary-to-primary pitch is 10,000 nm. (These were the masks used to generate Figures 1 and 2.)

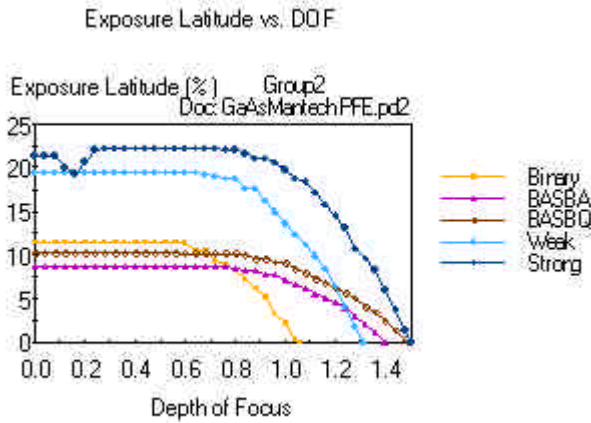


Figure 4 Exposure Latitude vs. Depth of Focus

The simulations were made with PROLITH's lumped parameter model (FINLE Technology, Inc.), with parameters of 0.5 NA, 365 nm wavelength, 0.3 sigma, contrast of 23, film thickness of 700 nm, absorbance of 0.2 per micron and diffusion length of 10nm. Results are shown in the following table.

Table 1: Exposure Latitude Summary Table

| Mask Type       | Illuminator         | 5% EL | DoF @ % ExpLat |
|-----------------|---------------------|-------|----------------|
| Strong          | 0.3 sigma           | 1.4   | 1.25 @ 10%     |
| Weak            | 0.3 sigma           | 1.2   | 1.0 @ 10%      |
| Binary w/Assist | Quad (0.62/0.2)     | 1.3   | 0.8 @ 9.6%     |
| Binary w/Assist | Annular (0.65/0.55) | 1.2   | 0.6 @ 8.7%     |
| Binary w/Assist | 0.7 sigma           | 1.0   | 0.7 @ 10.4%    |

The strong phase-shift mask yielded the best result, with a depth of focus of 1.4 $\mu$ m with concurrent 5% exposure latitude for  $\pm 10\%$ CD control. It was followed, in order, by the weak shifter, the binary with assist features using quadrupole illumination, then the binary with assist features using annular illumination, and finally, the binary mask. The concerns in using the masks with assist features are preventing the resist from printing the assists and maintaining a large center lobe to side lobe ratio by properly manipulating Equations 2 or 3.

## CONCLUSIONS

In conclusion, 365 nm lithography of discrete isolated features to form 250 nm devices can be obtained using optical resolution enhancement techniques. For 248 nm lithography 130 nm features are shown to be possible, but this is not the limit. Of the dark-field imaging techniques described, the strong-shifted GaAsMask shows the largest operating window. Which process is chosen depends on the process budget of the manufacturer and the adaptability of the exposure tool. For older exposure tools, in which off-axis illumination can be problematic due to field non-uniformities, conventional on-axis illumination would require GaAsMask for robust processing.

## ACKNOWLEDGEMENTS

The authors would like to thank Chris Mack of FINLE Technologies, Inc. and Fung Chen of ASML MaskTools for their helpful discussions, and FINLE Technologies, Inc. for the use of PROLITH and PROData.

## REFERENCES

[1] J. Petersen, *Analytical Description of Antiscattering and Scattering Bars*, Proceedings of SPIE Volume: 4000, pp 77-89, Optical Lithography XIII, Christopher J. Proglor, ed. July, 2000.